

## Effect of Entrance Geometry on the Capillary Flow of Cellulose Acetate-Acetone Solution

F. C. CHEN, *Research Laboratories, Tennessee Eastman Company, Division of Eastman Kodak Company, Kingsport, Tennessee 37662*

### Synopsis

Capillary flow data were obtained for a 27.5% solution of cellulose acetate in acetone. The solution temperature was 50°C, and the range of apparent shear rates investigated was  $1.7 \times 10^5$  to  $1.7 \times 10^6$  sec<sup>-1</sup>. Capillaries having tapered entrance angles of 37.88° to 120.63° were used. A power-law model was adequate to describe the shear stress at the wall ( $\tau_w$ ) and the corrected shear rate ( $\dot{\gamma}$ ) relationship. Entrance angle affected the entrance pressure drop corrected for kinetic energy, ( $\Delta P_{0,c}$ );  $\Delta P_{0,c}$  increased as the angle widened. Treating the entrance flow as an elongational flow situation facilitated superposition of the  $\Delta P_{0,c}$  data on a single curve. Estimated elongational viscosities decreased with increasing applied stress.

### INTRODUCTION

Although a capillary rheometer presents some difficulties in the exact analysis of the data obtained, it is by far the most common, or sometimes the only available, instrument for investigating the flow properties of polymeric materials at high shear rates. Geometric variables generally considered are capillary diameter and length; entrance geometry is not as frequently regarded as a variable. The effect of entrance geometry on the reliability of rheological data, therefore, remains a relatively unexplored problem.

Kamide et al.<sup>1</sup> reported that for a polypropylene melt, the end correction coefficient showed a minimum with a capillary having a 20° tapered entrance. For a poly( $\epsilon$ -caprolactam) melt, however, varying the entrance angle from 20° to 100° did not affect the correction coefficient.<sup>1</sup> Another study by Kamide<sup>2</sup> revealed that a 60° tapered entrance resulted in a minimum correction coefficient for a polyethylene melt. In contrast to these studies, Boles and Bogue<sup>3</sup> observed, at high shear rate, little or no change in the measured pressure drops on capillaries having entry cone angles of 21.6° to 180°. Results of all these studies suggest that the significance of entrance geometry in capillary rheometry may depend on the materials being investigated. Necessarily, such a statement is speculative. More experimental data for a variety of polymeric materials are required.

The present work deals with the capillary flow of a concentrated solution of cellulose acetate in acetone. Flow data were obtained at 50°C and at

apparent shear rates of  $1.7 \times 10^5$  to  $1.7 \times 10^6 \text{ sec.}^{-1}$  Short capillaries with conical entrance angles of  $37.88^\circ$  to  $120.63^\circ$  were used. Emphasis was placed on the effect of the entrance angle on the entrance pressure drop and on the possibility of treating the entrance flow as an elongational flow situation.

### EXPERIMENTAL

The apparatus to obtain the pressure drop data consisted of a supply tank, a gear pump (Zenith, size 2), a heat exchanger, and a set of capillaries. Figure 1 is a schematic diagram of the capillary geometry. Dimensions of

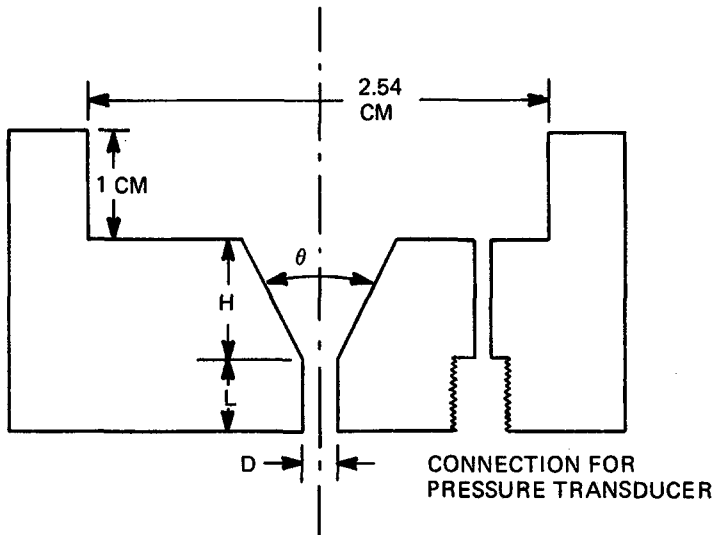


Fig. 1. Schematic diagram of capillary.

TABLE I  
Dimensions of Capillaries

Capillary series	$\theta$ , deg	$H$ , cm	$L$ , cm	$D$ , cm	$L/D$
I	42.73	0.3018	0.0201	0.0171	1.17
	37.88	0.2913	0.0406	0.0173	2.35
	38.25	0.3444	0.0762	0.0172	4.43
II	61.83	0.3208	0.0241	0.0172	1.40
	61.37	0.3396	0.0775	0.0182	4.26
	61.23	0.3233	0.1512	0.0180	8.40
III	89.80	0.3353	0.0165	0.0156	1.06
	89.80	0.3381	0.0780	0.0172	4.53
	89.83	0.3354	0.1575	0.0179	8.90
IV	120.63	0.3150	0.0076	0.0179	0.42
	120.63	0.3289	0.0213	0.0174	1.22
	120.42	0.3241	0.0782	0.0176	4.44
	120.45	0.3290	0.1643	0.0182	9.03

the capillaries are given in Table I. A Dynisco-pressure transducer (Model PT-110-1M) with a range of 0 to 1000 psig, together with a millivolt recorder, was employed to measure the pressure drop. An iron-Constantan thermocouple was used to measure the solution temperature which was controlled at  $50 \pm 1^\circ\text{C}$ .

The solution was 27.5% cellulose acetate<sup>4</sup> (Tennessee Eastman Co. E-394) in acetone. Average acetyl content of the acetate was 39.4%.

## RESULTS AND DISCUSSION

Figure 2 shows the relationship between the measured pressure drop  $\Delta P_T$  and the apparent shear rate  $\dot{\gamma}_a$ . The  $\dot{\gamma}_a$  was computed from the following expression:

$$\dot{\gamma}_a = 4Q/\pi R^3 \quad (1)$$

where  $Q$  is the volumetric flow rate and  $R$  is the capillary radius. The data in Figure 2 were used to plot  $\Delta P_T$  versus  $L/D$ , as illustrated in Figure 3. The data from Figure 3 were used to obtain shear stress at the wall  $\tau_w$  and the entrance pressure drop  $\Delta P_0$ . Results of calculations are given in Table II. Also included in this table are other calculated quantities which will be discussed later.

TABLE II  
Experimental Flow Data, Fluid Temperature at  $50 \pm 1^\circ\text{C}$

Capillary series	$\dot{\gamma}_a$ , $10^{-5}$ $\text{sec}^{-1}$	$\tau_w$ , psi	$\eta$ , poise	$\Delta P_0$ , psi	$\Delta P_{0,c}$ , psi	$\Delta KE/\Delta P_0$ , %	$\dot{\gamma}_a \left[ (\ln A^2 - \ln B^2) \left( \frac{R}{H} \right) \right]$ $10^{-5} \text{ sec}^{-1}$
I	2.0	4.3	1.04	100	98	2	0.25
	4.0	6.0	0.73	145	138	5	0.48
	8.0	8.3	0.50	227	198	13	0.92
	11.0	9.8	0.43	295	240	19	1.22
	15.0	14.4	0.46	370	267	28	1.56
	17.0	15.6	0.44	455	323	29	1.74
II	1.8	4.8	1.29	90	88	2	—
	3.5	5.5	0.76	150	144	4	0.56
	6.8	6.2	0.44	250	227	9	0.96
	9.8	8.0	0.48	325	278	14	1.35
	12.0	10.0	0.40	385	315	18	1.62
	15.0	13.2	0.42	465	355	24	1.95
III	2.3	5.8	1.22	110	108	2	0.37
	4.0	6.5	0.79	165	158	4	0.66
	7.0	8.0	0.55	255	234	8	1.12
	10.0	9.5	0.46	340	297	13	1.72
	12.0	10.9	0.44	392	329	16	1.85
	15.0	12.5	0.40	480	382	20	2.24
IV	1.7	5.8	1.65	100	99	1	—
	3.2	6.5	0.98	155	150	3	0.66
	6.0	8.6	0.69	245	227	7	1.21
	9.0	9.5	0.51	330	291	12	1.77
	12.0	10.5	0.42	450	380	16	2.31

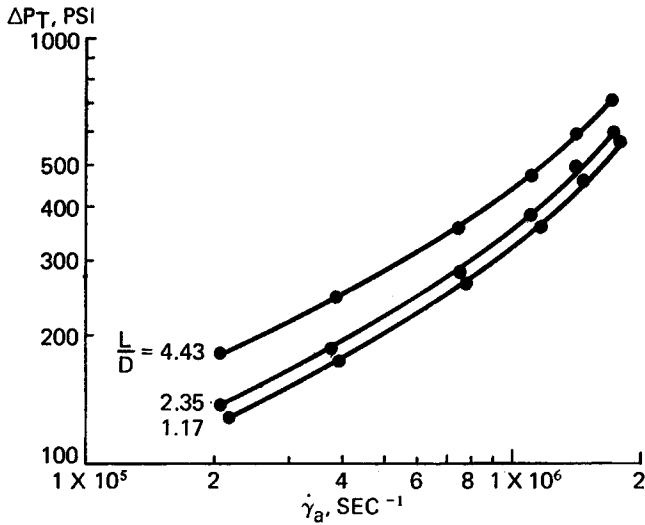


Fig. 2. Relationship between  $\Delta P_T$  and  $\dot{\gamma}_a$  data obtained with series 1 capillaries.

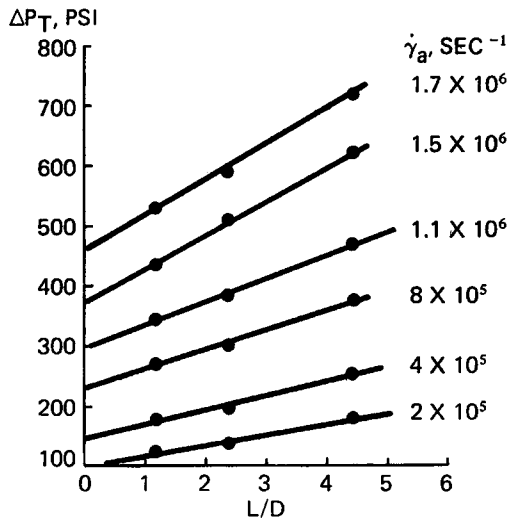


Fig. 3. Relationship between  $\Delta P_T$  and  $L/D$  data obtained with series 1 capillaries.

### Viscous Behavior

Figure 4 is a plot of  $\tau_w$  versus  $\dot{\gamma}$ , the corrected shear rate which relates to  $\dot{\gamma}_a$  by the following expression<sup>5</sup>:

$$\dot{\gamma} = \frac{3n + 1}{4n} \dot{\gamma}_a \quad (2)$$

where  $n = d(\log \tau_w)/d(\log \dot{\gamma}_a)$ . Figure 4 indicates that the viscous behavior of the solution of cellulose acetate in acetone is describable by a

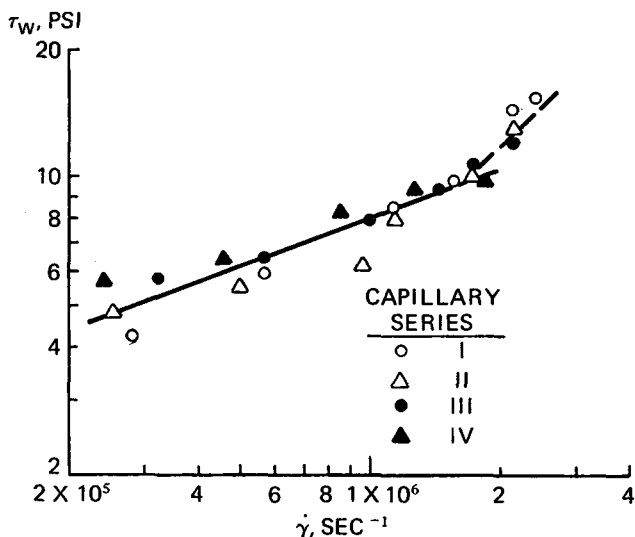


Fig. 4. Viscous behavior of cellulose acetate-acetone solution.

power-law model, at least within a range of shear rates from  $2.5 \times 10^5$  to  $1.7 \times 10^6 \text{ sec.}^{-1}$ . The equation obtained is

$$\tau_w = 4.82 \times 10^{-2} (\dot{\gamma})^{0.37} \text{ psi} \quad (3)$$

$$2.5 \times 10^5 < \dot{\gamma} < 1.7 \times 10^6 \text{ sec.}^{-1}.$$

At shear rates higher than  $1.7 \times 10^6 \text{ sec.}^{-1}$  (or  $\dot{\gamma}_a = 1.2 \times 10^6 \text{ sec.}^{-1}$ ), the fluid appears to be Newtonian; Newtonian behavior is suggested by the slope of  $\log \tau_w$  versus  $\log \dot{\gamma}$  which is equal to unity. Such behavior cannot be substantiated because of the limited quantity of experimental data and the error involved in data reduction.

The data from Table II show that viscosities of the solution were less than 1.65 poises at the shear rates investigated. The same fluid when measured at  $\dot{\gamma} = 1 \text{ sec.}^{-1}$  showed a value of 700 poises, indicating a strong dependence of viscosity on shear rate. Such a phenomenon was also reported by Smith,<sup>6</sup> who investigated the flow behavior of a concentrated solution of cellulose acetate in acetone.

Another interesting behavior of this fluid is that at the shear rates investigated,  $\tau_w$  amounted to less than 6% of  $\Delta P_0$ , the entrance pressure drop.

### Entrance Pressure Drop

According to Philippoff and Gaskins,<sup>7</sup>  $\Delta P_0$  includes the contributions from viscous end effect, elastic recovery, and kinetic energy. Kinetic energy loss was estimated from the following relationship:

$$\text{kinetic energy loss} = m\rho V^2 \quad (4)$$

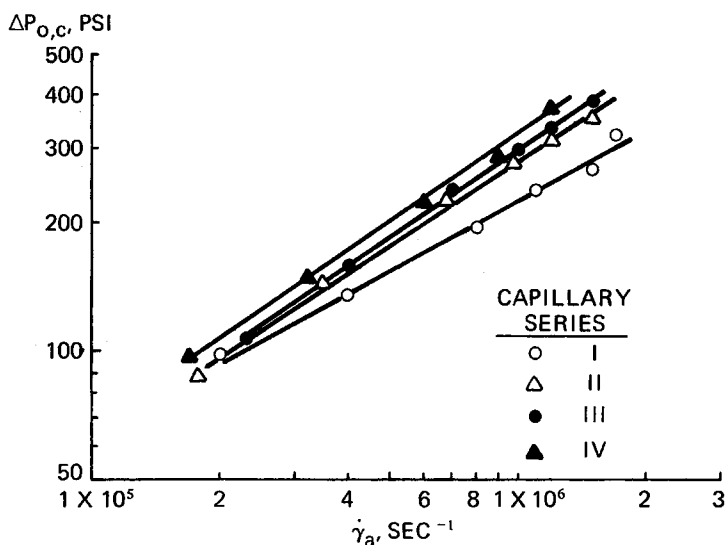


Fig. 5. Effects of entrance cone angle and apparent shear rate on  $\Delta P_{0,c}$ .

where  $m$  is a correction factor,  $\rho$  is the solution density (0.89 g/cc), and  $V$  is the average linear velocity. The correction factor  $m$  is related to  $n$  as follows<sup>8</sup>:

$$m = 3(3n + 1)^2 / [(4n + 2)(5n + 3)]. \quad (5)$$

As shown in Table II, the kinetic energy loss was substantial; it accounted for as much as 29% of  $\Delta P_0$ .

The applicability of eq. (5) to flow through short capillaries ( $L/D < 10$ ) is questionable, since a fully developed velocity profile may not have been established. However, as Figure 3 indicates and as Bagley's<sup>9</sup> data on polyethylene melts showed, the flow along the capillary length is the same at  $L/D = 0.42$  as at  $L/D = 9.03$  (see Table I). Although such evidence still does not justify the use of eq. (5), it is believed that this equation provides the best estimate.

In contrast to kinetic energy correction, viscous end effect and elastic recovery are not readily obtainable. Some approaches, such as those of Boles and Bogue,<sup>3</sup> Sutterby,<sup>10</sup> Oka,<sup>11</sup> and Tanner,<sup>12</sup> may be applicable. However, each of these approaches has some limitations: the fluid must be inelastic, or the cone angle must be small, or the shear rate must be less than  $10^4 \text{ sec}^{-1}$ . Therefore, in order not to introduce additional uncertainties, the entrance pressure drop corrected for kinetic energy,  $\Delta P_{0,c}$ , was examined for its change resulting from variation in the cone angle.

Figure 5 is a plot of  $\Delta P_{0,c}$  versus  $\dot{\gamma}_a$ . The influence on  $\Delta P_{0,c}$  of cone angle is evidenced. The trend is similar to that observed by Kamide et al.<sup>1</sup> for a polypropylene melt. From the data it is apparent that the choice of entry angle in capillary rheometry is an important factor, as was tacitly implied by Schott<sup>13</sup> and Metzner et al.<sup>14</sup>

TABLE III  
Jet Expansion Data

$\dot{\gamma}_a, 10^{-5} \text{ sec}^{-1}$	$B^2$
2	2.1
4	2.4
8	3.0
11	3.5
15	4.4
17	4.7

The effect of cone angle on  $\Delta P_{0,c}$  may be a result of fluid elasticity and/or elongational flow. The solution flowing through the entry cone undergoes an elongational deformation, and the elastic component of this deformation may be recovered as extrudate swelling. With this concept, Cogswell<sup>15</sup> derived an equation which permits estimation of elongational viscosity  $\eta_e$  from data of convergent flow. The equation of Cogswell can be rewritten as

$$\Delta P_{0,c} = \frac{1}{4} \eta_e \left( \frac{\ln A^2 - \ln B^2}{H/R} \right) \dot{\gamma}_a \quad (6)$$

where

$$A = 1 + \frac{H}{R} \tan \left( \frac{\theta}{2} \right) \quad B = \frac{\text{extrudate radius}}{R}$$

Physically,  $\ln A^2$  represents the total strain, and  $\ln B^2$  equals the elastic strain. Difference between these two, then, is the viscous strain. Equation (6) suggests that a log-log plot of  $\Delta P_{0,c}$  versus  $\left[ (\ln A^2 - \ln B^2) \left( \frac{R}{H} \right) \right] \dot{\gamma}_a$  should yield a straight line.

Jet expansion data for the solution of interest are given in Table III. The technique used by Paul<sup>16</sup> was followed to obtain the data; a capillary with a 60° entry angle was used. In reality, the quantity  $B^2$  can vary with the angle of entry. For lack of additional data, the values listed in Table III were assumed to be applicable to the analysis used in this work.

Figure 6 shows the results of the analysis. Normalization of  $\Delta P_{0,c}$  is fairly good. Slope of the straight line is 0.67. The equation fitted to the data is

$$\Delta P_{0,c} = 9.43 \times 10^{-2} \left[ \left( \frac{\ln A^2 - \ln B^2}{H/R} \right) \dot{\gamma}_a \right]^{0.67} \quad \text{for } 37^\circ < \theta < 120^\circ \quad (7)$$

Comparison of eq. (6) with eq. (7) suggests that  $\eta_e$  is stress dependent. This is illustrated in Figure 7, which indicates that  $\eta_e$  decreases with increasing  $\Delta P_{0,c}$ . Cogswell<sup>15</sup> observed similar behavior with polypropylene and poly-(4-methyl-1-pentene).

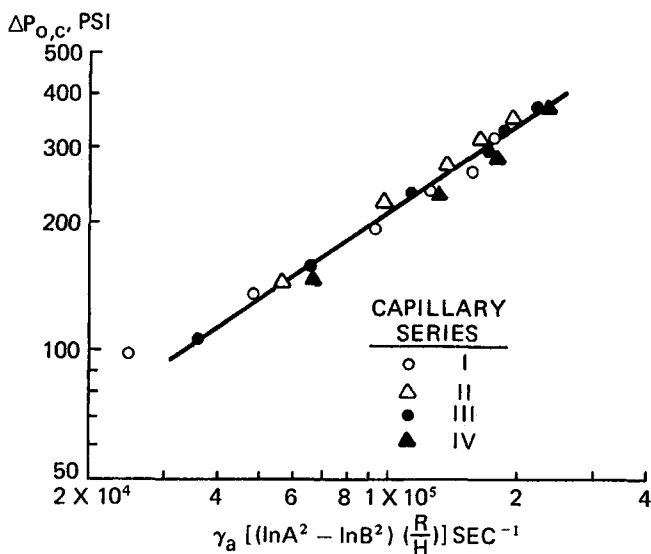


Fig. 6.  $\Delta P_{O,c}$  as a function of modified shear rate.

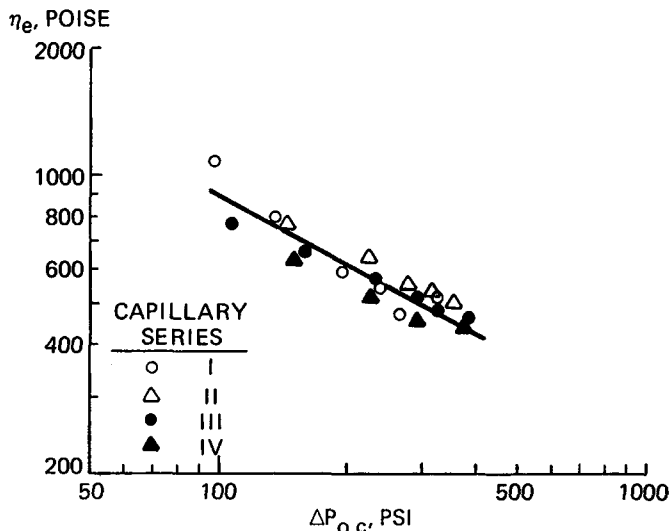


Fig. 7. Stress dependence of  $\eta_e$ .

### CONCLUSIONS

The flow data of a 27.5% solution of cellulose acetate in acetone were obtained at 50°C and at apparent shear rates of  $1.7 \times 10^5$  to  $1.7 \times 10^6$   $\text{sec}^{-1}$ , using capillaries having conical entries of 37.88° to 120.63°. Viscous properties of this solution were describable by a power-law model. Some indication of Newtonian behavior was observed at apparent shear rates greater than  $1.2 \times 10^6$   $\text{sec}^{-1}$ .



$\Delta P_{0,c}$  was seen to vary with the cone angle; it decreased as the angle decreased. Normalization of  $\Delta P_{0,c}$  with respect to cone angle was possible by considering the flow in a cone as elongational flow. Estimated elongational viscosities decreased with increasing applied stress.

In general, entrance geometry is not considered as a primary variable in capillary rheometry. The present work in support of other work<sup>1,2,13</sup> reveals the probable error that can result from such consideration.

### Notation

$A$	total strain, dimensionless
$B$	ratio of extrudate radius to capillary radius, dimensionless
$D$	capillary diameter, cm
$H$	length of cone-shaped entrance to capillary, cm
$\Delta KE$	pressure loss due to kinetic energy loss, psi
$L$	length of capillary, cm
$m$	kinetic energy loss correction factor from eq. (4), dimensionless
$n$	flow correction factor, dimensionless
$\Delta P_0$	experimental entrance pressure drop, psi
$\Delta P_{0,c}$	entrance pressure drop, corrected for kinetic energy, psi
$\Delta P_T$	total pressure drop across capillary, psi
$Q$	volumetric flow rate, cc/sec
$R$	capillary radius, cm
$V$	average linear velocity, cm/sec

### Greek Letters

$\dot{\gamma}_a$	apparent shear rate, sec <sup>-1</sup>
$\dot{\gamma}$	corrected shear rate, sec <sup>-1</sup>
$\tau_w$	wall shear stress, psi
$\eta$	viscosity, poises
$\eta_e$	elongational viscosity, poises
$\rho$	solution density, g/cc
$\theta$	cone-shaped capillary entrance angle, degrees

The author expresses his sincere thanks to Messrs. J. W. Johnson and C. R. Carr for performing the experimental work.

### References

1. K. Kamide, Y. Inamoto, and K. Ohno, *Kobunshi Kagaku*, **22**, 410 (1965).
2. K. Kamide and K. Fujii, *Kobunshi Kagaku*, **24**, 465 (1967).
3. R. L. Boles and D. C. Bogue, *SPE Tech. Pap.*, **15**, 119 (1969).
4. R. E. Boy, Jr., R. M. Schulken, Jr., and J. W. Tamblyn, *J. Appl. Polym. Sci.*, **11**, 2453 (1967).
5. J. M. McKelvey, *Polymer Processing*, Wiley, New York, 1962, p. 69.
6. T. L. Smith, *J. Polym. Sci.*, **14**, 37 (1954).
7. W. Philippoff and F. H. Gaskins, *Trans. Soc. Rheol.*, **2**, 263 (1958).
8. A. B. Metzner, *Advan. Chem. Eng.*, **1**, 77 (1956).
9. E. B. Bagley, *J. Appl. Phys.*, **28**, 624 (1957).

10. J. L. Sutterby, Ph.D. Thesis, University of Wisconsin, 1964.
11. S. Oka, *Japan. J. Appl. Phys.*, **6** (4), 423 (1967).
12. R. I. Tanner, *Ind. Eng. Chem., Fundam.*, **5** (1), 55 (1966).
13. H. Schott, *J. Polym. Sci. A*, **2**, 3791 (1964).
14. A. B. Metzner, J. L. White, and M. M. Denn, *Chem. Eng. Progr.* **62** (2), 81 (1966).
15. F. N. Cogswell, *Rheol. Acta*, **8** (2), 187 (1969).
16. D. R. Paul, *J. Appl. Polym. Sci.*, **12**, 2273 (1968).

Received October 22, 1971